NH_4^+, Na^+, K^+, and Ca^{2+} and salts of CO_3^{2-} and SO_4^{2-} (*13*). This ammoniated water is inferred to react with anhydrous silicates and produce the ammoniated hydrous mineral(s) observed in spectrum of Ceres.

The identification of an ammonium-bearing mineral species, most likely ammoniated saponite, on the surface of Ceres implies that the secondary temperatures cannot have exceeded 400 K. Studies on the stabilities of ammoniated phyllosilicates indicate that the deammoniation of most samples begins at temperatures of ~400 K (*16*). The deammoniation of a phyllosilicate is spectrally detected by decreased intensity and wavelength shifts of the fundamental NH absorptions. The wavelength position of the NH_4^+ absorption on Ceres is similar to that of samples that have not been heated to greater than 400 K. This observation implies that Ceres has experienced minimal thermal reprocessing. Difficulties in obtaining high resolution data with a high signal-to-noise ratio, such as that obtainable with the CGAS spectrometer, for small asteroids with low albedos may be inhibiting identification of additional ammonium-bearing asteroids.

REFERENCES AND NOTES

1. M. J. Gaffey *et al.*, in *Asteroids II*, R. P. Binzel, T. Gehrels, M. S. Matthews, Eds. (Univ. of Arizona Press, Tucson, 1989), pp. 98–127.
2. D. R. Davis *et al.*, in *ibid.*, pp. 805–826.
3. L. A. Lebofsky *et al.*, *Icarus* **48**, 453 (1981).
4. We obtained data using the Cooled Grating Array Spectrometer (CGAS) with a 32 linear array InSb detector and the D grating with a resolution of 0.013 μm. Observing conditions were good during the nights the data were obtained. The reference standards included the moon and the solar analog star Lambda Auriga. Full terrestrial atmospheric extinction corrections were applied to the data [as described in R. N. Clark *et al.*, *J. Geophys. Res.* **95**, 14463 (1990); R. N. Clark and T. B. McCord, *Publ. Astron. Soc. Pac.* **91**, 571 (1979)].
5. M. A. Feierberg *et al.*, *Geochim. Cosmochim. Acta* **95**, 971 (1981).
6. F. Van Olphen and J. J. Fripiat, *Data Handbook for Clay Materials and Other Nonmetallic Minerals* (Pergamon, New York, 1979).
7. C. E. Weaver and L. D. Pollard, *The Chemistry of Clay Minerals* (Elsevier, New York, 1975).
8. M. Zolensky and H. Y. McSween, Jr., in *Meteorites and the Early Solar System*; J. F. Kerridge and M. S. Matthews (Univ. of Arizona Press, Tucson, 1988), pp. 114–143.
9. T. D. Jones, thesis, University of Arizona (1988).
10. F. P. Fanale and J. R. Salvail, *Icarus* **82**, 97 (1989).
11. B. Hapke, *J. Geophys. Res.* **86**, 3039 (1981).
12. W. M. Calvin and R. N. Clark, *Icarus* **89**, 305 (1991).
13. J. S. Lewis and R. G. Prinn, *Planets and Their Atmospheres* (Academic Press, New York, 1984).
14. ______, *Astrophys. J.* **238**, 357 (1980).
15. R. G. Prinn and M. B. Fegley, *Annu. Rev. Earth Planet. Sci.* **15**, 171 (1987).
16. B. Chourabi and J. J. Fripiat, *Clays Clay Minerals* **29**, 260 (1981).

17. This work was supported by NASA Planetary Geology and Geophysics Program (W17077 to T.V.V.K. and W15805 to R.N.C.). T.V.V.K., R.N.C., W.M.C., and R.H.B. were Visiting Astronomers at NASA's Infrared Telescope Facility.

13 November 1991; accepted 3 February 1992

The Effect of Surface Roughness on Triton's Volatile Distribution

ROGER V. YELLE

Calculations of radiative equilibrium temperatures on Triton's rough surface suggest that significant condensation of N_2 may be occurring in the northern equatorial regions, despite their relatively dark appearance. The bright frost is not apparent in the Voyager images because it tends to be concentrated in relatively unilluminated facets of the surface. This patchwork of bright frost-covered regions and darker bare ground may be distributed on scales smaller than that of the Voyager resolution; as a result the northern equatorial regions may appear relatively dark. This hypothesis also accounts for the observed wind direction in the southern hemisphere because it implies that the equatorial regions are warmer than the south polar regions.

TRITON'S SOUTHERN HEMISPHERE IS characterized by normal albedos of 0.8 to 0.9 (*1*) and hemispheric albedos of ~0.8 (*2*). This observation, combined with ground-based measurements of spectral features attributed to N_2 and CH_4 (*3*), strongly suggests that Triton's southern hemisphere is covered with bright N_2 and CH_4 frost. Triton's northern hemisphere is characterized by normal albedos of 0.6 to 0.7 (*1*) and hemispheric bond albedos of 0.5 to 0.6 (*2*). Surface temperatures calculated from regional hemispheric albedos imply that the atmosphere, which is in vapor pressure equilibrium with the surface, should be condensing at most northern latitudes, and thus that the surface should be covered with fresh frost (*3*). Why then is the northern hemisphere darker than the southern hemisphere?

Lunar and Planetary Laboratory, University of Arizona, Tucson, AZ 85721.

Spencer (*4*), on the basis of an analogy with the Martian southern polar cap (*5*), suggested that frost in the northern hemisphere has been darkened by exposure to sunlight. Moore and Spencer (*6*) suggested that the northern hemisphere appears relatively dark because the N_2 frost has metamorphosized into large transparent ice blocks. This latter view was supported by Eluszkiewicz (7) who argued that sintering may create an annealed, transparent nitrogen layer. Both of these hypotheses predict that the south polar and northern equatorial regions of Triton should be buffered to a single temperature by the process of frost sublimation (*8*). However, temperatures inferred from wind directions imply that the equatorial regions are warmer than the south polar regions (*9*). For this to occur some of Triton's northern hemisphere must be devoid of N_2 frost. Thus, it seems likely that the northern hemisphere is warmer and darker than the southern polar cap because of the presence of exposed patches of bare ground, which have a lower albedo than that of fresh frost. Bare ground in this context refers to the underlying surface, which may be composed of water-rich ices that have been darkened by interaction with ultraviolet radiation or energetic particles (*10*).

Here, I adopt as a hypothesis that fresh frost is bright and bare ground relatively dark and explore a mechanism for reconciling the observed albedo pattern and wind directions with the expectation that frost will condense in the cold northern hemisphere. The basic idea is that large-scale albedo patterns can be influenced by small-scale topography. Surface roughness can alter the solar energy deposition over areas smaller than the resolution in Voyager images (roughly 1 km for the highest resolution images) and so affect the distribution of N_2 frost. Areas on the surface that are relatively cold because of their orientation with respect to the sun will also be more difficult to see; thus, bright patches of fresh frost may be hidden. When viewed at low resolution, this type of terrain will have an average albedo that is lower than that of fresh frost and an average temperature larger than the frost temperature. I refer to this effect as small-scale cold trapping.

If frost is bright and bare ground dark, then the southern hemisphere is covered with a large polar cap, whereas in the recent past the northern equatorial region was nearly bare but is now being slowly covered with frost in an inhomogeneous (patchy) manner. Presumably, these are seasonal effects. It was late southern spring on Triton during the Voyager flyby, and the southern polar cap, which was formed in the previous winter, had not had time to evaporate fully. Similarly, all the frost in the northern equatorial regions might have sublimated during the southern winter and spring. The north-

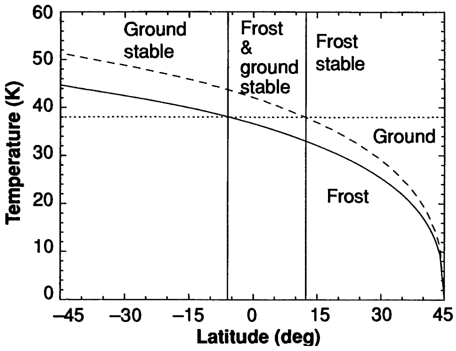

Fig. 1. Zones of frost and bare ground stability on Triton. The calculations use a hemispheric albedo of 0.8 for frost and 0.5 for bare ground with emissivities of 0.66 and 0.95, respectively. Diurnal averaged solar energy deposition is assumed.

ern equatorial regions only recently became cool enough to permit frost condensation.

Evidence for the small-scale cold-trapping hypothesis comes from Voyager photometry, which has been used to derive an average surface roughness of 10° (*11*). As I show below, slopes of this magnitude are sufficient to alter local sublimation rates. However, this roughness is based on the disc-integrated brightness of Triton, and the northern equatorial regions may have different photometric properties than the disc average. In addition, photometric parameters were derived with the assumption that the surface had a homogeneous composition, which may not be the case. This assumption is discussed further below. The cold-trapping hypothesis is also supported by analogy with Mars, where small-scale cold-trapping of H_2O ice was observed by the Viking 2 lander (*12*).

Assuming that topography has a negligible effect on the energy balance of the surface, I calculated zonally averaged frost sublimation rates based on hemispheric albedos derived from Voyager data (*2*). I used hemispheric albedos of 0.5 and 0.8 and emissivities of 0.95 and 0.66 for bare ground and fresh frost, respectively. The latter emissivity value is derived from the observed atmospheric pressure with some assumptions about the size of the southern and northern polar caps (*2*). I assumed that the frost temperature is 38 K, consistent with the atmospheric pressure of 13 to 19 μbar (*13*). As shown in Fig. 1, the surface can be divided into three regions. Southward of −6°, the solar energy deposition rates are large, causing sublimation in frost-covered areas and inhibiting condensation on bare ground. Northward of 13° the solar energy deposition rates are small, and the radiative equilibrium temperatures of smooth bare ground are less than 38 K; therefore, bare ground at these latitudes is unstable and should be quickly covered by frost. Both frost and bare ground are stable between latitudes of −6° and 13°. The greatest variations of surface brightness are also seen in this latitude band (*2, 14*); this observation gives some support to the hypothesis that bare ground is dark and frost bright.

Surface temperatures attributed to radiative equilibrium and the stability of zones of frost and bare ground can be profoundly affected by relatively mild slopes in the northern hemisphere. Solar insolation varies as the cosine of the zenith angle, which is close to zero in the northern equatorial regions, and is very sensitive to small changes in the slope of the terrain. Consider a small area of surface illuminated by the sun at an angle of 82°. For a hemispheric albedo of 0.5 and an emissivity of 0.95, the radiative equilibrium temperature of the surface is $T_e = 37$ K; thus, frost will condense. Moreover, a surface that is tilted 5° toward the sun has a radiative equilibrium temperature of $T_e = 42$ K, whereas a surface tilted 5° away from the sun has $T_e = 29$ K and consequently will be buffered to the frost temperature of 38 K. Therefore, at low illumination angles, the sunny slopes of mild hills should be devoid of frost while the northern slopes should have frost.

For the cold-trapping hypothesis to be valid, roughness and frost patches must be present on scales small compared with the resolution of the Voyager images (~1 km), but there is also a lower limit determined by the properties of the surface. Because two patches of ground in close proximity will share energy, the lower limit to the roughness scale length is set by the thermal conductivity of the surface. The scale length over which thermal conduction can alter the surface temperature can be defined by $L = k\Delta T/F$, where k is the thermal conductivity, F is the flux of energy conducted from the bare patches to frosted patches, and ΔT is the temperature difference between the patches. For a 10° difference in slope at a solar incidence angle of 82°, $\Delta T = 3$ K, and $k = 2 \times 10^{-1}$ W m^{-1} K^{-1} (*15*) implies that $L = 5$ cm.

Eventually the frost layer will become thick enough to cover surface topography. The frost deposition rate in the northern hemisphere is on the order of 1 cm per earth year for a density of 1 g/cm^3 (*4*). Condensation has been occurring in the northern equatorial regions for approximately 10 years; as a result, the frost deposits in shadowed regions should be ~10 cm thick. Both this estimate and the thermal conduction calculation suggest that topographical relief with significant slopes (~10°) must be present at scales significantly larger than 10 cm for the cold-trapping hypothesis to be correct.

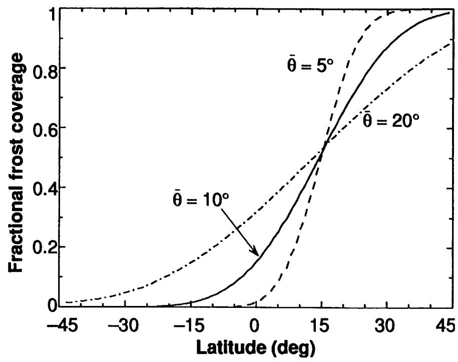

Fig. 2. Fraction of surface that is frost-covered as a function of latitude. The emissivities and albedos used in this calculation are the same as in Fig. 1.

Diurnally averaged radiative equilibrium calculations for a rough surface predict that a substantial part of the northern hemisphere is devoid of frost. To calculate this fraction I modeled the surface as having a Gaussian distribution of slopes (*11, 16*),

$$f(\theta) = \exp\left(-\frac{1}{\pi}\frac{\tan^2(\theta)}{\tan^2(\bar{\theta})}\right)\sec^2(\theta)\sin(\theta) \tag{1}$$

where $\bar{\theta}$ is the average slope of the surface, and calculated radiative equilibrium temperatures for each facet of the surface. For the uncertain cases where either frost or bare ground would be stable, I assumed that the surface is in fact bare, because of the seasonal effects discussed earlier. For a smooth surface, the fraction of surface covered by frost would change discontinuously from 1 to 0 at a latitude of 13°N (Fig. 1). With surface roughness included, the transition is gradual (Fig. 2). At 13°N, 53% of the surface area is covered with frost, and even as far as 25°N, ~25% of the surface is bare for $\bar{\theta} = 10°$. The average surface temperature will also vary smoothly and reaches a value of 40 K at 13°N, although individual facets may have temperatures as high as 48 K (Fig. 3).

The prediction that the average temperature is higher than the frost temperature agrees with the inference from the wind directions that the equatorial regions must be hotter than the south polar region, which is covered with frost and must be at 38 K. Of course, the relevant quantity for meteorological considerations is the atmospheric temperature not the surface temperature. The surface temperature will vary over relatively short distances, and I assumed that some horizontal mixing will take place so that the atmospheric temperature is approximately equal to the average surface temperature.

The small-scale cold-trapping hypothesis can also explain the relatively low reflectivity of the northern hemisphere. To calculate the

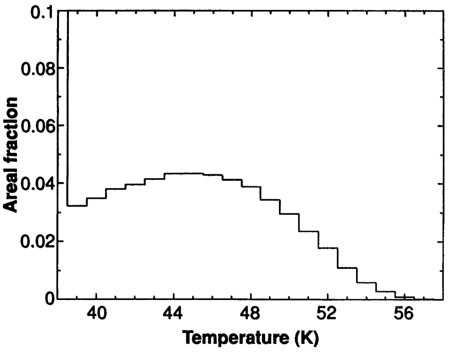

Fig. 3. The distribution of temperature over the surface at 13°N latitude. The emissivities and albedos used in this calculation are the same as in Fig. 1.

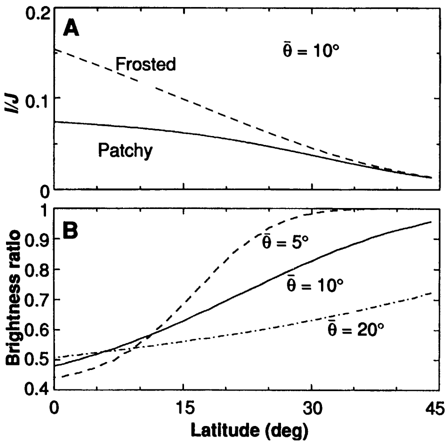

Fig. 4. (**A**) The variation of reflected intensity (I), normalized by the solar flux (J), as a function of latitude for a phase angle of 35°. The scattering function in Eq. 2 is used to calculate energy deposition with ω = 0.996 for frosted regions and ω = 0.90 for bare ground; g = −0.28 is used for both types of surface. (**B**) The ratio of intensity of reflected light from a patchy surface to the intensity from a frost-covered surface for roughness parameters of $\bar{\theta}$ = 5°, 10°, and 20°.

surface brightness of Triton as a function of latitude I again assumed that surface slopes have a Gaussian distribution and calculated the surface brightness by a numerical integration over the distribution, taking into account the visibility of each facet. The scattering on each facet of the surface is assumed to be described by a reflectivity of the form (*16*)

$$r(\mu, \mu_0, \alpha) = \frac{\omega}{4\pi} \frac{\mu_0}{\mu + \mu_0} [P(g, \alpha) + H(\omega, \mu)H(\omega, \mu_0) - 1] \quad (2)$$

where $H(\omega, \mu)$ is the two-stream approximation to the H functions and $P(g, \alpha)$ is the Henyey-Greenstein phase function with asymmetry parameter g and phase angle α. Following Hillier *et al.* (*11*), I used g = −0.28 and ω = 0.996 for the frosted regions. Because much of the disc-integrated intensity comes from the south polar cap, I assumed that these values are appropriate for N_2 frost. However, it is not clear that fresh frost in the northern hemisphere would have the same photometric properties as that forming the southern polar cap. More uncertain are the photometric parameters for the bare ground. I arbitrarily used the same asymmetry parameter for the bare ground and frost and adopted a single scattering albedo of ω = 0.90. These values imply that hemispheric albedos are 0.8 for frost and 0.5 for bare ground for a solar incidence angle of 75°.

To calculate the reflected intensity, I assumed that the viewer is over the subsolar meridian at a latitude of −13°. The phase angle for this geometry is 35°. These values are roughly consistent with those for the best Voyager images of the northern hemisphere. The latitudinal variation of surface irradiance was calculated by averaging the contributions from each facet of the surface (Fig. 4A). Each facet was treated as bare ground or frost covered depending upon its radiative equilibrium temperature. The scattering and temperature calculations were based upon Eq. 2 with the scattering parameters listed above. The brightness is significantly decreased for $\bar{\theta}$ = 10° and 20° over most of the visible northern hemisphere (Fig. 4B). The brightness is decreased beyond that expected from the fraction of area that is frost covered because the brightness and temperature of the sunlit slopes are coupled. The slopes that are easiest to see will also tend to be warm and hence devoid of frost.

The hypothesis presented here should be testable through detailed analysis of the Voyager images. The calculations demonstrate that there is a tendency for the brightness of the patchy terrain to decrease more slowly with latitude than either frosted or completely bare terrain. The increase in fractional frost coverage with latitude partially offsets the general decrease in brightness due to the increase of emission angle with latitude. It may be difficult to separate changes in brightness due to partial frost coverage from changes caused by illumination geometry, but an analysis of the images with the small-scale cold-trapping hypothesis in mind might be able to simultaneously determine the scattering function and surface roughness. This would provide an important consistency check and may be a critical test for the viability of this hypothesis.

Perhaps the most serious uncertainty in the model is the use of the roughness parameter in photometric theory to characterize the surface slopes on Triton. It is unclear how this roughness parameter relates to the topographical roughness on Triton. On the other hand, slopes on the order of 10° appear to be reasonable. Topography is apparent on kilometer scales in the Voyager images of Triton (*1*), suggesting that the surface may be quite rough below the resolution limit. The relaxation rates of small-scale topography are sufficiently slow that little decay should occur over the age of the solar system (*17*).

In the surface temperature calculations, I have neglected internal heat flow because it has a small effect on the movement of frost over a single Triton season. For example, if all of Triton's internal heat were focused into the northern hemisphere, the frost stability boundary shown in Fig. 1 would move northward by only 2°. However, internal heat is important over longer time scales (*18*) and may help to explain the absence of a large permanent polar cap in the northern hemisphere.

REFERENCES AND NOTES

1. B. A. Smith *et al.*, *Science* **246**, 1422 (1989).
2. J. A. Stansberry, *Geophys. Res. Lett.* **16**, 1773 (1989).
3. D. P. Cruikshank, R. H. Brown, R. N. Clark, *Icarus* **58**, 293 (1984); D. P. Cruikshank, R. H. Brown, L. P. Giver, A. T. Tokunaga, *Science* **245**, 283 (1989).
4. J. A. Spencer, *Geophys. Res. Lett.* **16**, 1769 (1989).
5. D. A. Paige and A. P. Ingersoll, *Science* **228**, 1160 (1985).
6. J. M. Moore and J. A. Spencer, *Geophys. Res. Lett.* **17**, 1757 (1990).
7. J. Eluszkiewicz, *J. Geophys. Res.* **96**, 19217 (1991).
8. L. M. Trafton [*Icarus* **58**, 312 (1984)] demonstrated that methane frost would be buffered by a methane atmosphere to a constant temperature. Ingersoll (*9*) provided quantitative justification for this assumption of N_2 on Triton.
9. A. P. Ingersoll, *Nature* **344**, 315 (1990).
10. W. R. Thompson and C. Sagan, *Science* **250**, 415 (1990).
11. J. Hillier *et al.*, *ibid.*, p. 419.
12. T. Svitek and B. Murray, *J. Geophys. Res.* **95**, 1495 (1990).
13. G. L. Tyler *et al.*, *Science* **246**, 1466 (1989).
14. A. S. McEwen, *Geophys. Res. Lett.* **17**, 1765 (1990).
15. The conductivity used in this calculation is taken from T. A. Scott [*Phys. Rep.* **27**, 3 (1976)] and is appropriate for N_2 ice. The conductivity of solid methane is a factor of 2 as large [V. G. Manzheli and I. N. Krupskii, *Soviet Phys. Solid State* **10**, 221 (1968)].
16. B. Hapke, *J. Geophys. Res.* **86**, 3039 (1981); *Icarus* **59**, 41 (1984).
17. The Rayleigh-Taylor time constant for viscous relaxation of topography is given by the inverse of the strain rate, which I obtain from J. Eluszkiewicz and D. J. Stevenson [*Geophys. Res. Lett.* **17**, 1753 (1989)]. From their figure 1, I estimated a strain rate of 10^{-18} s^{-1} for relief of 1 m, implying a relaxation time of 10 billion years for topography supported by methane ice.
18. R. H. Brown, T. V. Johnson, J. D. Goguen, G. Schubert, M. N. Ross, *Science* **251**, 1465 (1991).

19. I would like to acknowledge interesting conversations with A. Ingersoll, J. Eluszkiewicz, B. Murray, and D. Stevenson. This research was supported by National Aeronautics and Space Administration grants NAGW 2360 and NAGW 2017 to the University of Arizona. I am grateful to Y. Yung and the Division of Geological and Planetary Sciences at the California Institute of Technology for providing a stimulating environment in which to write this paper.

17 October 1991; accepted 31 January 1992